Effects of various substrate materials on structural and optical properties of amorphous silicon nitride thin films deposited by plasma-enhanced chemical vapor deposition

Liangyi Hang (杭良毅)*, Weiguo Liu (刘卫国), and Junqi Xu (徐均琪)**

Shaanxi Provincial Key Laboratory of Thin Films Technology and Optical Test, Xi'an Technological University, Xi'an 710021, China

**Corresponding author: lyhang999@163.com; **corresponding author: wgliu@163.com*

Received April 2, 2020; accepted June 10, 2020; posted online July 13, 2020

The plasma-enhanced chemical vapor deposition (PECVD) technique is well suited for fabricating optical filters with continuously variable refractive index profiles; however, it is not clear how the optical and structural properties of thin films differ when deposited on different substrates. Herein, silicon nitride films were deposited on silicon, fused silica, and glass substrates by PECVD, using silane and ammonia, to investigate the effects of the substrate used on the optical properties and structures of the films. All of the deposited films were amorphous. Further, the types and amounts of Si-centered tetrahedral Si–Si_vN_{4-v} bonds formed were based upon the substrates used; Si–N_4 bonds with higher elemental nitrogen content were formed on Si substrates, which lead to obtaining higher refractive indices, and the Si–SiN_3 bonds were mainly formed on glass and fused silica substrates. The refractive indices of the films formed on the different substrates had a maximum difference of 0.05 (at 550 nm), the refractive index of SiN_x films formed on silicon substrates was 1.83, and the refractive indices of films formed on glass were very close to those formed on fused silica. The deposition rates of these SiN_x films are similar, and the extinction coefficients of all the films were lower than 10^{-4}.

Keywords: thin films; plasma-enhanced chemical vapor deposition; optical properties; structural properties; substrate materials.

doi: 10.3788/COL202018.083101.

Plasma-enhanced chemical vapor deposition (PECVD) is an excellent technique for fabricating antireflection films and optical filters. The PECVD technique can be used to prepare photoelectrical films of silicon nitride (SiN_x)[1,2], silicon oxynitride[3,4], silicon carbonitride[5,6], and fluorinated silica[7,8]. These films are transparent in the visible (Vis) near-infrared region, exhibit good wear resistance, high stability, high surface hardness, and a high degree of densification, and thus are used in various applications[9–13]. The PECVD technique is currently one of the preferred deposition methods for the SiN_x films due to a lower thermal budget than other chemical vapor deposition techniques, which are known as a low-temperature (lower than 400°C) deposition technique. Further, the dielectric constant[14] and chemical components[15,16] of the thus-deposited SiN_x films can be controlled readily by adjusting the deposition parameters; the variable range of the refractive index is 1.83–2.06, and the extinction coefficient is lower than 10^{-3}[17]. Therefore, the amorphous SiN_x films were widely used in the field of optics; for instance, they can be used as optical waveguide materials in integrated optics[18], biorecognition layers of biosensors in biological applications[19], and antireflection films and passivation layers in photovoltaics for improving the photoelectric conversion efficiency[20]. More importantly, the adjustable refractive index[21], low-absorption, and amorphous state of the SiN_x films make them particularly attractive for use as optical thin films, especially films that exhibit a gradient in their refractive index[22]. Thus, SiN_x films, which can be considered as a tailored high refractive index structure, are expected to play a crucial role in many applications and devices.

For the advantages mentioned above, SiN_x films deposited by the PECVD technique, were chosen as a high refractive index material to design and to deposit complex optical filters with a gradient refractive index profile, such as broadband antireflection filters, notch filters, and laser protection filters. Besides, SiN_x films can be deposited on a Si substrate with SiO_2 nanostructures as an optical microstructure device to improve the imaging properties of the optical field. All of these applications are related to the effects of various substrates on SiN_x films; this is why we need to do this study.

Several researchers have reported that the optical properties and microstructures of thin films are affected by the material properties of the substrate used[23–26]. For example, the radio frequency (RF) magnetron sputtering technique was used to synthesize indium gallium nitride (InGaN) crystalline films on n- and p-type Si substrates. It was found that the choice of the substrate material had a significant effect on the optical, morphological, and structural characteristics of the InGaN films[24]. Other researchers used the same method to deposit zinc oxide (ZnO) crystalline films onto Si, sapphire, polyethylene

 © 2020 Chinese Optics Letters

terephthalate (PET), and polypropylene carbonate substrates and found that the ZnO crystalline films formed on the PET substrates showed better optical and structural characteristics[25]. These reports suggest that the material properties of the substrate used affect those of the deposited thin films, including their optical characteristics and structures. However, few researchers have studied the influence of substrates on the optical properties of amorphous SiN_x films deposited by PECVD at present. Therefore, to improve the manufacturing accuracy of SiN_x optical films and to clarify the differences in the characteristics of the films deposited on various substrates, it is necessary to study the effects of various substrates on the optical and structural characteristics of films.

In this Letter, the SiN_x films were deposited by the PECVD technique using silane (SiH_4) and ammonia (NH_3) gases on Si, fused silica (FS), and glass substrates. The structural and optical properties of the films in the Vis near-infrared region were measured. We used the chemical bond configurations to analyze the changed refractive index of SiN_x films. By analyzing these results, the effects of various substrates on the structural and optical properties of the films were clarified, which can be referenced by other researchers.

SiN_x thin films were deposited by the RF-PECVD technique on a p-type crystalline (100) single-polished Si substrate with a thickness of 500 μm (10 mm × 10 mm), FS substrate with a thickness of 2 mm (Φ 25 mm), and glass substrate with a thickness of 1 mm (Φ 30 mm). All the experiments were performed in a class 1000 cleanroom. The substrates were cleaned with a mixture of ethanol and ether (3:1) and then heated for 10 min. Finally, the dried substrates were placed in the vacuum chamber of the coating system. The coating system used was a typical flat-plate PECVD (RF 13.56 MHz) system (PD-220 N™, SAMCO). The upper plate of the chamber had many holes with different sizes and is called the shower plate. All reactive gases were fully mixed through the shower plate before they entered the chamber. Figure 1 shows a schematic diagram of the RF-PECVD coating machine. Before the

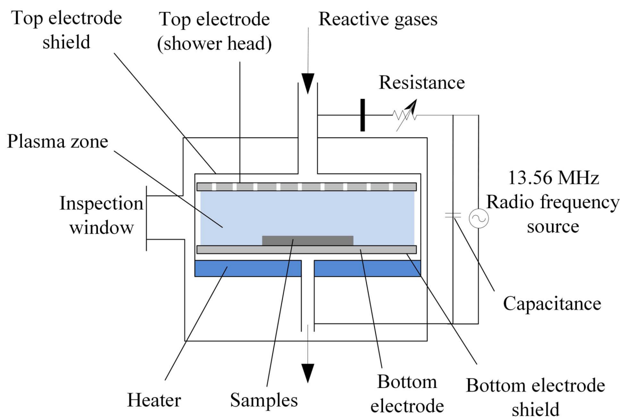

Fig. 1. Schematic of RF-PECVD coating system used in this study.

depositing process, the base pressure of the chamber was 8×10^{-3} Pa, and all the substrates were heated at least 40 min, which means that all the substrates were heated uniformly, avoiding the thermal gradient effects caused by the difference in the sample thickness. The films were deposited at a temperature of 250°C, chamber pressure of 100 Pa, deposition time of 6 min, and RF power of 200 W, and the flow rates of SiH_4 (10% in Ar) and NH_3 (purity, 99.999%) were 60 sccm (standard cubic centimeters per minute). For convenience, the SiN_x thin films formed at Si, glass, and FS substrates were named SiN_{x1}, SiN_{x2}, and SiN_{x3}, respectively.

X-ray diffraction (XRD) using a diffractometer (Advance-D8, Bruker) equipped with a Cu K_α radiation source having $\lambda = 1.5406 \times 10^{-10}$ m was performed to determine the crystalline states of the films. The X-ray photoelectron spectroscopy (XPS) (K-Alpha, Thermo Fisher) was used to analyze the relative atomic composition and the chemical bonding configuration formed within the various films. XPS measurements were performed using monochromatized X rays from an Al K_α source (1486.6 eV). The sample surface was etched using a 2 keV Ar ion beam with a current of 10 mA applied for 30 s. The spectra were analyzed and processed using the Thermo Avantage software. All the XPS spectra were corrected for any charging effects by fixing the C 1s binding energy (BE) at 284.8 eV and were subjected to Shirley background subtraction. The experimental data were evaluated using the Powell fitting algorithm and Gauss–Lorentz peak shape. The BE scale was referenced from the BE database, which can provide enough information about the chemical composition of the samples.

An ultraviolet (UV)-Vis spectrophotometer (Lambda 950, Perkin Elmer) was used to measure the transmittances of the films formed on the glass and FS substrates. The refractive indices, extinction coefficients, and physical thicknesses of the films were determined from a spectroscopic ellipsometer (M-2000UI, J. A. Woollam) using the Cauchy model. The optical film design software TFCalc was used to establish the "air/films/substrate/air" model for fitting the transmittance values of the thin films formed on Si substrates.

The XRD patterns of the non-stoichiometric SiN_x thin films formed on different substrates are shown in Figs. 2(a) and 2(b). Figure 2(a) shows the XRD patterns of the SiN_{x1} thin films formed on the p-type crystalline (100) single-polished Si substrates. It can be seen that all the samples exhibit a strong peak at the same 2θ value. However, this peak is not attributable to the SiN_{x1} films but is related to the Si substrate (100) itself. Figure 2(b) shows the XRD patterns of the SiN_x thin films formed on the glass and FS substrates. No peak related to a crystal plane was observed; this was in keeping with previous reports[27]. In addition, it is known that as-deposited PECVD films often contain substantial amounts of bonded hydrogen, and that these films are more properly described as hydrogenated SiN_x films[28,29]. In this regard, PECVD SiN_x films are both structurally undefined (amorphous)

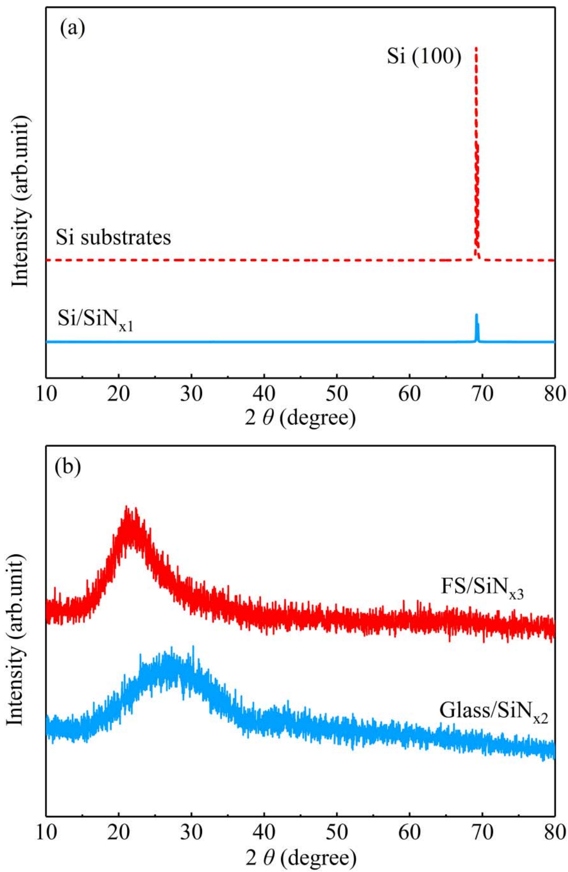

Fig. 2. XRD patterns of SiN_x thin films formed by PECVD method on (a) Si and (b) glass and fused silica (FS).

and chemically undefined (non-stoichiometric)[2,30,31]. Therefore, it is confirmed that the films deposited on all three substrates were amorphous.

Table 1 shows the relative atomic concentrations of elemental Si and N in the SiN_x films. The concentrations are the semi-quantitative test results; the uncertainty is ±4% for XPS results because of some variations in the composition depending on the depth of the analysis within the layer. It can be found that the relative atomic concentrations of Si and N of all the SiN_x films are similar, and the concentration of elemental Si in the SiN_{x1} is slightly higher than that of other elements.

In order to analyze the chemical bond configurations of amorphous and non-stoichiometric SiN_x films, two models are commonly used to describe the bonds: random bonding model (RBM) and random mixture model (RMM). RBM and RMM are based on the Si-centered tetrahedrons with in-plane triply coordinated N as bonding structures[32].

Figures 3(a) and 3(b) are the Si 2p and N 1s high-resolution XPS spectra of the SiN_x films, respectively, and G represents the glass substrate. Figure 3(a) shows the BE values of the Si 2p main peaks for all the SiN_x films are greater than that for Si (99.60 eV)[33] and less than that for Si_3N_4 (102.40 eV)[34], which means the Si–N chemical bond configurations with different types and amounts of Si-centered tetrahedron bonds were formed inside the films[35]. The XPS Si 2p spectra do not exhibit a low-energy peak near 99.60 eV related to elemental Si, suggesting that no Si–Si bonds or Si clusters were formed in these films. Besides, the results in Fig. 3(a) show that the BE value of the Si 2p main peak of the SiN_x films deposited on the Si, FS, and glass substrates decreased gradually from 101.90 eV to 101.70 eV, indicating that the relative concentration of elemental N in the SiN_{x1} films was higher than that in other films[36]. Figure 3(b) shows that the BE values of elemental N 1s main peaks for all the SiN_x films varied from 397.50 eV to 397.86 eV, which correspond to the BE values for different non-stoichiometric SiN_x films[37]. The atomic-level non-equilibrium mixtures were generated in the plasma of the reactive gas during

Table 1. Relative Atomic Concentrations of Si and N of SiN_x Films Deposited on Various Substrates, Obtained by XPS

Samples	Silicon (%)	Nitrogen (%)	Uncertainty (%)
SiN_{x1}	48	52	±4
SiN_{x2}	46	54	±4
SiN_{x3}	46	54	±4

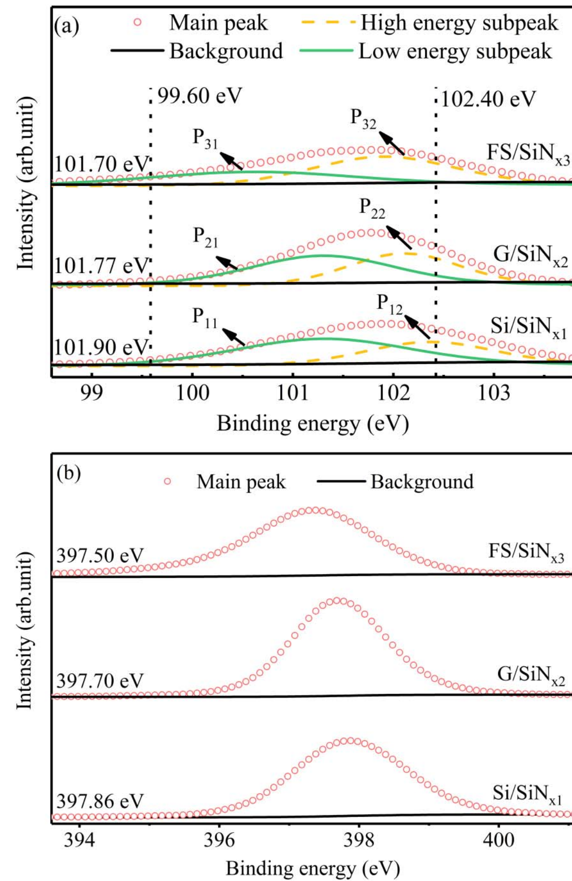

Fig. 3. High-resolution XPS spectra of SiN_x films formed on Si, glass (G), and FS substrates: (a) Si 2p spectra; (b) N 1s spectra.

Table 2. Binding Energies of All the Possible Chemical Bonds in Regions Si 2p

No.	Tetrahedron	Bonding Unit	$E_B{}^a$ (eV) of Si 2p
1	Si–Si_3N	Si_3N	100.30
2	Si–Si_2N_2	Si_3N_2	101.00
3	Si–SiN_3	SiN	101.70
4	Si–N_4	Si_3N_4	102.40

$^a E_B$ represents the value of BE.

the deposition process, further, in order to determine the types of the Si–N bonds formed in the samples, the typical Si-centered tetrahedron Si–$Si_vN_{(4-v)}$ ($v = 0, 1, 2, 3, 4$) bond configurations were used for analysis. The chemical bond configurations based on Si-centered tetrahedrons were most likely to be formed inside the SiN_x films that are shown in Table 2[32,38].

Figure 3(a) shows that the main compounds of the SiN_x films formed on FS, glass, and Si substrates were gradually changed from SiN (101.70 eV) to Si_3N_4 (102.40 eV). The BE values of two subpeaks in Si 2p high-resolution spectra of the SiN_{x1} films were 101.30 eV (P_{11}) and 102.34 eV (P_{12}). For the SiN_{x2} and SiN_{x3} films, the BE values of two subpeaks were 101.30 eV (P_{21}), 102.10 eV (P_{22}), 100.60 eV (P_{31}), and 101.90 eV (P_{32}). It is indicated that more Si–Si_3N, Si–Si_2N_2, and Si–SiN_3 bonds were formed in the SiN_{x2} and SiN_{x3} films, while the Si–N_4 bonds were formed in the SiN_{x1} films. In addition, the BE values of the two subpeaks in the SiN_{x3} films deposited on FS substrates are smallest, indicating that the Si-centered tetrahedral bonds with higher Si concentration were formed in the SiN_{x3} films.

The XPS results show that various Si-centered tetrahedral bonds were formed by the elemental Si and N in the SiN_x films, which corresponded to various compounds (i.e., Si–N_4 for Si_3N_4 and Si–SiN_3 for SiN). Different compounds exhibit different dielectric constants and densities. As a result, the refractive indices and film thicknesses of the SiN_x films were different. Compared with the SiN_{x2} and SiN_{x3} films deposited on the glass and FS substrates, the SiN_{x1} films deposited on the Si substrates displayed Si-centered tetrahedral structures with a higher N content, because of which their properties were similar to those of Si_3N_4 films. This meant that, under the deposition parameters, the refractive index of the SiN_{x1} films formed on the Si substrates was greater than those of the films formed on the FS and glass substrates; Ref. [39] shows the same results.

The optical constants of the SiN_x films were determined by the ellipsometry measurements. According to the previous experimental results obtained by the laboratory team, indicating that the extinction coefficients were far less than the refractive indices of the amorphous SiN_x films, thus, the Cauchy model was used to fit the optical constants. Figures 4(a) and 4(b) show the refractive indices and extinction coefficients of all the SiN_x films formed on various substrates, respectively. At the wavelength of 550 nm, the results of refractive indices show that the maximum deviation is 0.05; the value of the refractive index of the SiN_{x1} films deposited on Si substrates is 1.83, which is higher than those of SiN_{x2} and SiN_{x3} films; the values of refractive indices of the SiN_{x2} and SiN_{x3} films are very similar, so the deviation is only 0.01, and this kind of deviation also can be seen in Ref. [39]. Figure 4(b) shows that the extinction coefficients of all the SiN_x films are small, which are less than the order of magnitude of 10^{-4}. It has been reported that the very low absorption is mainly caused by the amorphous hydrogenated form of SiN_x films[28,29]. Therefore, the effect ($\Delta n = 0.05$) of various substrates on the refractive index of the SiN_x films is of critical importance with respect to the fabrication of optical multilayer films, for instance, the notch filters (with the number of layers ranging from one hundred[40] up to a few thousand[41]).

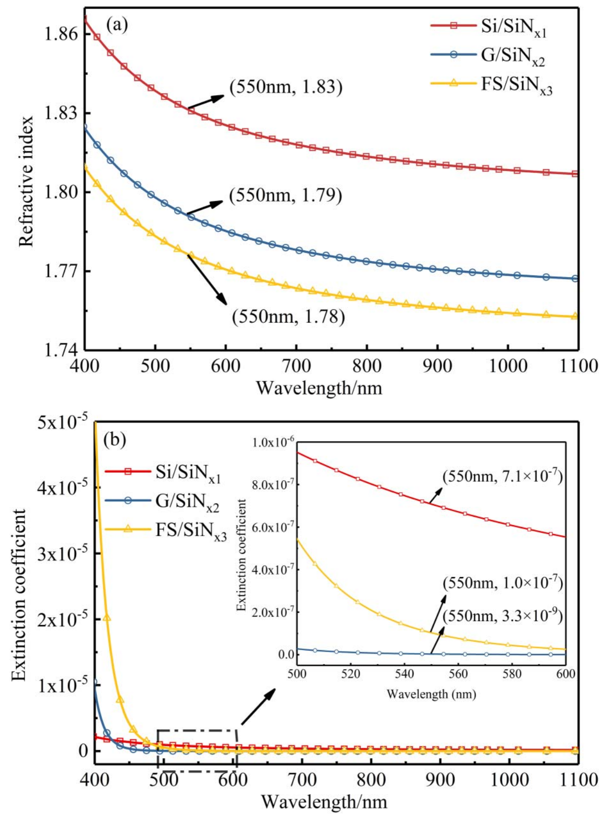

Fig. 4. Optical constants of SiN_x films formed on different substrates: (a) refractive index; (b) extinction coefficient.

Figure 5 shows the film thickness and deposition rate of the SiN_x films. According to our previous work, the results of the film thickness stay in the order of magnitude of 0.1, which means the accuracy is reliable and acceptable[17,42]. It is found that the deposition rates of the SiN_{x1}, SiN_{x2}, and SiN_{x3} films were 21.5, 21.7, and 20.9 nm/min, respectively, which presents that these substrates have less effect on the deposition rates of the amorphous SiN_x films.

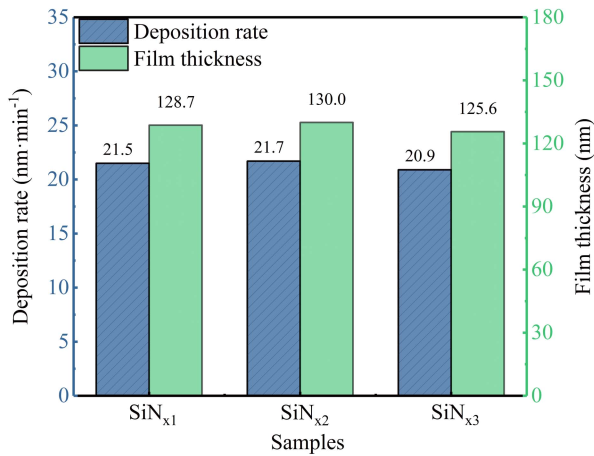

Fig. 5. Deposition rates and physical thicknesses of SiN_x films deposited on various substrates.

Figure 6 shows the transmittance of the SiN_x films. Figure 6(a) displays three curves: (1) the measured transmittance of the glass substrates (Glass substrates); (2) the measured transmittance of a SiN_{x2} film deposited on glass (Measured); (3) the simulated transmittance of a SiN_x film deposited on a glass substrate based on the measured optical constants of the films formed on Si substrates [Simulated (Si)]. The effects of Si and glass substrates on the transmittance of the films can be directly found by comparing this simulated transmittance with the measured transmittance. The transmittance of the SiN_x films formed on the glass and FS substrates will not be compared, due to the deviation of the refractive index between the SiN_{x2} and SiN_{x3} films being only 0.01 [according to Fig. 4(a)]; thus, these two kinds of substrates have less effect on the transmittance. Figure 6(b) shows the corresponding transmittance for SiN_{x3} films formed on FS substrates.

Figure 6 shows the measured transmittance spectra of the substrates and SiN_x films coincided at wavelengths

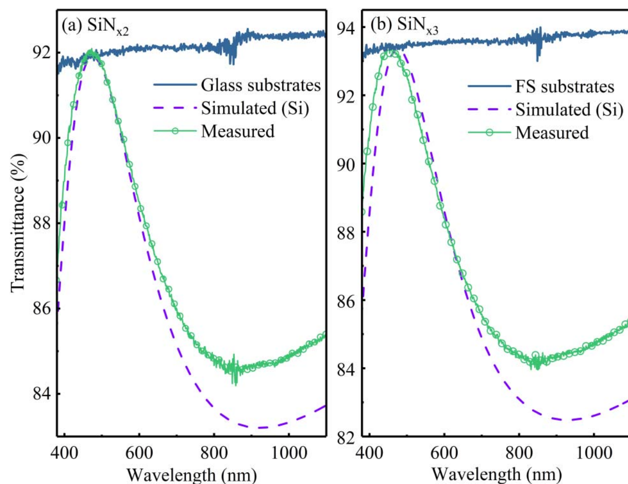

Fig. 6. Transmittances of SiN_x films: (a) SiN_{x2} on glass; (b) SiN_{x3} on FS.

that are integer multiples of $\lambda_0/2$, where λ_0 is the reference wavelength, indicating that the SiN_x films formed on the glass and FS substrates did not exhibit absorption[43]. This was consistent with the fact that the extinction coefficients of the films were close to zero. In addition, comparing with the measured transmittance, the calculated transmittance [Simulated (Si)] was shifted slightly. This was mainly owing to the fact that the film thickness of the films formed on various substrates was different; further, the depths of valleys differed due to the differences in the refractive indices. The transmittance deviation of the single-layer SiN_x film is greater than 1% at the minimum point, which has obviously exceeded the accuracy of the spectrophotometer ($\pm 0.3\%$).

In summary, SiN_x films were deposited by the PECVD technique on Si, glass, and FS substrates. The analyses of the structures of the SiN_x films showed that all the deposited films were amorphous. Si-centered tetrahedral $Si–Si_vN_{4-v}$ bonds were formed in the SiN_x films, and the $Si–N_4$ bonds forming in SiN_{x1} films deposited on the crystalline Si substrates, while the $Si–Si_3N$, $Si–Si_2N_2$, and $Si–SiN_3$ bonds formed in SiN_x films deposited on the amorphous substrates (glass and FS). The optical properties of the SiN_x films showed that the SiN_{x1} films have the maximum refractive indices (i.e., $n = 1.83$ at 550 nm) in the range of 400–1100 nm, and the SiN_{x3} films have the lower refractive indices (i.e., $n = 1.78$ at 550 nm). All of the SiN_x films displayed the properties of low absorption (the extinction coefficients are lower than 10^{-4}). These substrates have less effect on the deposition rates of the SiN_x films.

The PECVD technique is suitable for fabricating amorphous SiN_x films that show extremely low absorption in the Vis to near-infrared region. In this study, the types and amounts of chemical bond configurations in the SiN_x films were affected by the various substrates, which leads to the differences in the refractive indices. Thus, before designing and fabricating optical multilayer filters and devices, the effects of various substrate materials on structural and optical properties of amorphous SiN_x films should be paid attention.

Further work is to study the effects of various deposition parameters on the structural and optical properties of SiN_x films, such as reactive gas flow rates and temperatures.

This work was supported by the Project of Innovative Team of Advanced Optical Manufacturing and Detection (No. 2017KCT-08-02).

References

1. B. Karunagaran, S. J. Chung, S. Velumani, and E.-K. Suh, Mater. Chem. Phys. **106**, 130 (2007).
2. J. Jaglarz, M. Jurzecka-Szymacha, and S. Kluska, Thin Solid Films **669**, 564 (2019).
3. A. E. T. Kuiper, S. W. Koo, F. H. P. M. Habraken, and Y. Tamminga, J. Vac. Sci. Technol. B **1**, 62 (1983).
4. J. Dupuis, E. Fourmond, J. F. Lelièvre, D. Ballutaud, and M. Lemiti, Thin Solid Films **516**, 6954 (2008).

5. C. Huber, B. Stein, and H. Kalt, Thin Solid Films **634**, 66 (2017).
6. K. Olesko, H. Szymanowski, M. Gazicki-lipman, J. Balcerzak, W. Szymanski, W. Pawlak, and A. Sobczyk-guzenda, Mater. Sci. Poland 2018) 56 ,**36**).
7. M. D. Barankin, T. S. Williams, E. Gonzalez, and R. F. Hicks, Thin Solid Films **519**, 1307 (2010).
8. M. Abbasi-Firouzjah and B. Shokri, J. Appl. Phys. **114**, 214102 (2013).
9. V. Cech, J. Studynka, B. Cechalova, J. Mistrik, and J. Zemek, Surf. Coat. Tech. **202**, 5572 (2008).
10. A. Upadhyaya, M. Sheoran, and A. Rohatgi, in *Proceedings of the 31st IEEE Photovoltaic Specialists Conference and Exhibition* (2005), p. 1273.
11. T. Lauinger, J. Schmidt, A. G. Aberle, and R. Hezel, Appl. Phys. Lett. **68**, 1232 (1996).
12. A. del Prado, E. San Andrés, F. L. Martinez, I. Mártil, G. González-Daz, W. Bohne, J. Röhrich, B. Selle, and M. Fernández, Vacuum **67**, 507 (2002).
13. I. Koirala, C. Park, S. Lee, and D. Choi, Chin. Opt. Lett. **17**, 082301 (2019).
14. B. Rangarajan, A. Y. Kovalgin, K. Wörhoff, and J. Schmitz, Opt. Lett. **38**, 941 (2013).
15. M. F. Ceiler, Jr., P. A. Kohl, and S. A. Bidstrup, J. Electrochem. Soc. **142**, 2067 (1995).
16. I. Guler, Mater. Sci. Eng. B-Adv. **246**, 21 (2019).
17. J. Xue, L. Hang, and H. Liu, Opt. Tech. **40**, 353 (2014).
18. J. Dupuis, E. Fourmond, D. Ballutaud, N. Bererd, and M. Lemiti, Thin Solid Films **519**, 1325 (2010).
19. J. Seiffe, L. Weiss, M. Hofmann, L. Gautero, and J. Rentsch, in *Proceedings of the 23rd European Photovoltaic Solar Energy Conference 1700* (2008).
20. P. Li, L. Hang, J. Xu, and L. Li, J. Appl. Opt. **36**, 206 (2015).
21. W. Jiang, D. Xu, B. Xiong, and Y. Wang, Ceram. Int. **42**, 1217 (2016).
22. L. Hang, W. Liu, L. Hang, and S. Zhou, Laser & Optoelectron. Progress **57**, 130003 (2020).
23. A. Basak, A. Hati, A. Mondal, U. P. Singh, and S. K. Taheruddin, Thin Solid Films **645**, 97 (2018).
24. E. Erdoğan and M. Kundakçı, Microelectron. Eng. **207**, 15 (2019).
25. S. H. Ribut, C. A. C. Abdullah, and M. Z. M. Yusoff, Results Phys. **13**, 102146 (2019).
26. T. Jiang, R. Miao, J. Zhao, Z. Xu, T. Zhou, K. Wei, J. You, X. Zheng, Z. Wang, and X. Cheng, Chin. Opt. Lett. **17**, 020005 (2019).
27. B. Astinchap and K. G. Laelabadi, J. Phys. Chem. Solids **129**, 217 (2019).
28. W. A. Lanford and M. J. Rand, J. Appl. Phys. **49**, 2473 (1978).
29. G. Santana, J. Fandino, A. Ortiz, and J. C. Alonso, J. Non-Cryst. Solids **351**, 922 (2005).
30. W. R. Knolle and J. W. Osenbach, J. Appl. Phys. **58**, 1248 (1985).
31. J. Thurn, R. F. Cook, M. Kamarajugadda, S. P. Bozeman, and L. C. Stearns, J. Appl. Phys. **95**, 967 (2004).
32. P. Cova, S. Poulin, O. Grenier, and R. A. Masut, J. Appl. Phys. **97**, 073518 (2005).
33. P. J. W. Weijs, J. F. van Acker, J. C. Fuggle, P. A. M. van der Heide, H. Haak, and K. Horn, Surf. Sci. **260**, 102 (1992).
34. G. M. Ingo, N. Zacchetti, D. della Sala, and C. Coluzza, J. Vac. Sci. Tech. A **7**, 3048 (1989).
35. V. A. Gritsenko, R. W. N. Kowk, H. Wong, and J. B. Xu, J. Non-Cryst. Solids **297**, 96 (2002).
36. S. Naskar, S. D. Wolter, C. A. Bower, B. R. Stoner, and J. T. Glass, Appl. Phys. Lett. **87**, 261907 (2005).
37. J. R. Shallenberger, D. A. Cole, and S. W. Novak, J. Vac. Sci. Tech. A **17**, 1086 (1999).
38. N. Jehanathan, Y. Liu, B. Walmsley, J. Dell, and M. Saunders, J. Appl. Phys. **100**, 123516 (2006).
39. X. Zhang, "Research on anti-reflection coatings by PECVD technology," Master Thesis (Xi'an Technological University, 2010).
40. T. Begou, H. Krol, D. Stojcevski, F. Lemarchand, M. Lequime, C. Grezes-Besset, and J. Lumeau, CEAS Space J. **9**, 441 (2017).
41. K. Hendrix, Appl. Opt. **56**, C201 (2017).
42. H. Liu, L. Hang, and J. Xue, Opt. Instrum. **36**, 364 (2014).
43. H. A. Macleod, *Thin-Film Optical Filters* (CRC press, 2018).